# DETECTION OF THE 3RD HEART SOUND USING RECURRENCE TIME STATISTICS

*Christer Ahlstrom, Peter Hult, Per Ask*

Department of Biomedical Engineering
Linköping University, Linköping, Sweden
{chrah, pethu, peras}@imt.liu.se

**ABSTRACT**

The 3rd heart sound (S3) is normally heard during auscultation of younger individuals, but it is also common in many patients with heart failure. Compared to the 1st and 2nd heart sounds, S3 has low amplitude and low frequency content, making it hard to detect (both manually for the physician and automatically by a detection algorithm). We present an algorithm based on a recurrence time statistic which is sensitive to changes in a reconstructed state space, particularly for detection of transitions with very low energy. Heart sound signals from ten children were used in this study. Most S3 occurrences were detected (98 %), but the amount of false extra detections was rather high (7% of the heart cycles). In conclusion, the method seems capable of detecting S3 with high accuracy and robustness.

## 1. INTRODUCTION

Bioacoustic signals originate from mechanical processes in the body, and the heart sounds can be seen as fingerprints reflecting myocardial function. The 3rd heart sound (S3) is produced by rapid deceleration of the early transmitral flow and the associated vibration of the entire cardiac-blood pool (cardiohemic) system. The more rapid the deceleration of early transmitral flow, the more likely a 3rd heart sound will be present [1]. S3 occurs normally in children but disappear with increasing age. The sound can reappear in elderly persons and is clinically important because of its established connection with heart failure [2-4]. The sound is characterized by its low amplitude, short duration and low frequency, making it difficult to hear with a stethoscope (see Table I). The amplitude becomes stronger when the mass of the ventricular wall increases and when the stiffness of the wall decreases. The higher the velocity of the inflow to the ventricle will be, the higher the amplitude becomes [1]. An example of S3 is shown in Fig 1.

Using signal processing to clarify, visualize or classify heart sounds and murmurs have been a research topic for a long time [5], but automatic detection of S3 is still a new field of research. However, our group has previously developed a method based on a matched wavelet approach [2, 3].

TABLE I
FEATURES OF THE THIRD HEART SOUND[a]

| | |
|---|---|
| Frequency content: | 15 – 70 Hz. |
| Timing: | 0.12 – 0.18 s after closure of the semilunar valves or 0.45 ± 0.01 s after the R-peak in the ECG. |
| Duration: | 0.06 ± 0.01 s. |

[a]Reprint from [6].

The aim of this study was to evaluate a new method for S3 detection. Based on recent developments in the detection of weak transient signals, we track changes in the recurrence time statistics of the sound signal. If a change is detected in the time window where S3 is expected (0.12 – 0.18 s after closure of the semilunar valves or 0.45 ± 0.01 s after the R-peak in the ECG), it is interpreted as an S3 occurrence.

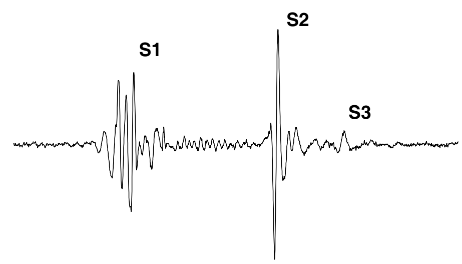


Fig. 1. Example of a heart sound signal where 1st, 2nd and 3rd heart sounds are marked.

## 2. PATIENTS AND DATA COLLECTION

Signals were recorded from ten healthy children (5 male, 5 female, mean age 10.5 years). The sounds were recorded by a contact accelerometer (Siemens, EMT 25C, Sweden) connected to a microphone amplifier (Siemens, E285E, Sweden). A standard 3-lead ECG was also recorded as a time reference (S&W, Diascope DS 521, Denmark). Both signals were digitized at 2.5 kHz with 12-bits per sample (National Instruments, DAQCard-700), after passing an anti-aliasing filter with a cut-off frequency of 1.25 kHz. Acquisition and processing of data were conducted in Labview (National Instruments, USA) and Matlab (The MathWorks, USA), respectively.

The signals were recorded in a soundproof room and the recording site was over the apex, the sensor was fixed with a belt around the body. 30 seconds of data was acquired during breath hold, and the presence of 3rd heart sounds was determined by visual inspection of the recordings (an S3 occurrence was marked if a signal component with low frequency was present in a time window 0.12 – 0.20 s after the 2nd heart sound).

## 3. METHODOLOGY

The dynamics of a time discrete system is determined by its possible states in a multivariate vector space (called state space or phase space). The transitions between the states are described by vectors, and these vectors form a trajectory describing the time evolution of the system. An observed signal S is a projection from this multivariate state space onto a one-dimensional time-series. S can be considered as a set of n scalar measurements,

$$S = \{s_1, s_2, ..., s_n\} \tag{1}$$

from which a sequence of N d-dimensional vectors $a_k$ can be constructed using Takens' delay embedding theorem

$$a_k = \{s_k, s_{k+\tau}, s_{k+2\tau}, ...s_{k+(d-1)\tau}\} \quad k = 1,2,..., N \tag{2}$$

where $\tau$ is a delay parameter and d is the embedding dimension [7]. The purpose of the embedding is to unfold the projection back into a reconstructed state space that is dynamically and topologically equivalent to the state space that generated the process S [8].

Takens' theorem assumes that S is infinitely long and noise free. These conditions are seldom met, and the selection of $\tau$ and d affects how accurately the embedding reconstructs the system's state space. When dealing with finite time series, the choice of embedding dimension is not too crucial if d is sufficiently large. A more important consideration is the window length needed to reconstruct each vector $a_k$, $w = \tau \cdot d$. Typically, univariate time series exhibit some sort of periodicity and w should be chosen to span several of these oscillations. In this study, $\tau$ and d were chosen based on the standard techniques of average mutual information and false nearest neighbors [7]. An average value of d was used for the whole study, while $\tau$ was calculated adaptively by automatic detection of the first minimum of the average mutual information.

### 3.2. Recurrence time statistics

Nonlinear dynamical systems theory has successfully been used to detect weak transient signals in noisy and nonstationary environments. Most of these methods are based on various measures of nearest neighbors in state space (neighbors indicate recurrence of states in state space). It has been shown that nearest neighbors in state space can be divided into true recurrence points and sojourn points [9], and in [10] two recurrence time statistics were introduced based on these two kind of recurrence points. An arbitrary state, $a_{ref}$, is chosen somewhere on the trajectory whereupon all neighboring states within a hypersphere of radius r are selected, see Fig. 2.

$$B_r(a_{ref}) = \{a : \|a - a_{ref}\| \le r\} \tag{3}$$

The recurrence points of the first kind (T1) are defined as all the points within the hypersphere (i.e. the entire set $B_r$). Since the trajectory stays within the neighborhood for a while (thus generating a whole sequence of points), T1 doesn't really reflect the recurrence of states. Therefore, the recurrence points of the second kind (T2), is defined as the first states entering the neighborhood in each sequence (these points are commonly called true recurrence points). T2 is hence the set of points constituted by $B_r(a_{ref})$ excluding the sojourn points, see Fig. 2. Both T1 and T2 are related to the information dimension via a power law, motivating their ability to detect weak signal transitions based on amplitude, period, dimension and complexity [10]. Specifically, T2 is able to detect very weak transitions with high accuracy, both in clean and noisy environments while T1 has the distinguished merit of being more robust to the noise level and not sensitive to the choice of r. A mathematically more rigorous definition of T1 and T2 can be found in [10].

A sliding window was used to partition the recorded signal into overlapping segments (and hence obtaining time resolution), where T1 and T2 are calculated for each segment.

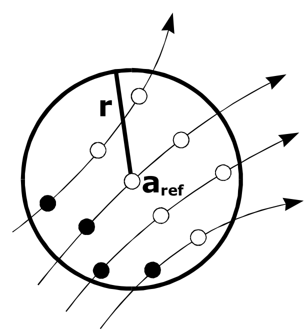


Fig. 2. Recurrence points of the second kind (solid circles) and the sojourn points (open circles) in $B_r(a_{ref})$. Recurrence points of the first kind comprise all circles in the set.

## 4. DETECTION OF S3

The complete data set consisted of 816 1st and 2nd heart sounds (408 heart cycles). The embedding dimension for state space reconstruction was found to be d = 6.6 ± 1.1, and d = 7 was used throughout the study. The delay parameter was allowed to vary since τ fluctuated heavily between 5 and 22. This calculation was done adaptively by automatic detection of the first minimum of the average mutual information.

In the calculation of recurrence time statistics, the r-value is an important parameter. If r is chosen too low, the hypersphere would be low on data and if r is chosen too high, the hypersphere will contain misleading information from erroneous parts of the reconstructed state space. T1 was calculated for a certain r-value, while T2 was calculated for a whole range of values.

The timing of the 1$^{st}$ and 2$^{nd}$ heart sounds were obtained by thresholding T1. In Fig. 3b, an example of T1 is shown for a whole range of r-values. T1 for a particular r-value (r = 0.4) is shown in Fig. 3c after normalization to unity. This latter curve was simply thresholded at 0.5 to obtain the 1$^{st}$ and 2$^{nd}$ heart sound occurrences. Our results were compared to an ECG to verify the detections. With r = 0.4, a detection accuracy of 99.5% was achieved, see Table II.

Due to its ability to detect very weak signals, T2 was used to find S3. T2 was calculated for r = [0.001 1], which resulted in a 2D image (Fig. 3d). This was converted to 1D by an edge detection algorithm and normalized to unity (Fig. 3e). The edge detection was implemented by simple lowpass filtering and detection of the maximum value in each column. In the 1D signal, occurrences of S3 were found by looking for a maximum within a time window defined as 0.10 − 0.30 s after the 1$^{st}$ and 2$^{nd}$ heart sound, respectively. If the amplitude of the maximum was one third higher than the base line level (calculated as the mean amplitude in the time window 0.30 − 0.70 s after the 1$^{st}$ and 2$^{nd}$ heart sound), the algorithm marked the peak as an S3 occurrence. To avoid the problems involved in discriminating between the 1$^{st}$ and 2$^{nd}$ heart sound, we searched for S3 within the predetermined time window following both of them. 97.9 % of the S3 occurrences were accurately detected, but the amount of false extra detections was rather high, see Table II.

TABLE II

RESULTS FROM THE AUTOMATIC DETECTION METHODS

| | |
|---|---|
| No. of heart cycles: | 408 |
| False positive heart sounds: | 2 |
| False negative heart sounds: | 0 |
| No. of S3: | 390 |
| No. of detected S3: | 382 |
| No. of false detected S3: | 29 |
| No. of missed S3: | 8 |

To accurately distinguish S3 from the other heart sounds may be a problem for the detection algorithm. However, S3 appears in a well defined time period within the heart cycle. This makes it possible to reject most of the false components, which appear in the part of the heart cycle where S3 is not expected. One limitation which contributes to false detection is that our algorithm doesn't distinguish between the 1$^{st}$ and 2$^{nd}$ heart sounds. Search for S3 is therefore performed after both the 1$^{st}$ and 2$^{nd}$ heart sounds. This limitation could be avoided by inclusion of an ECG signal, making it easy to differentiate between the 1$^{st}$ and 2$^{nd}$ sound.

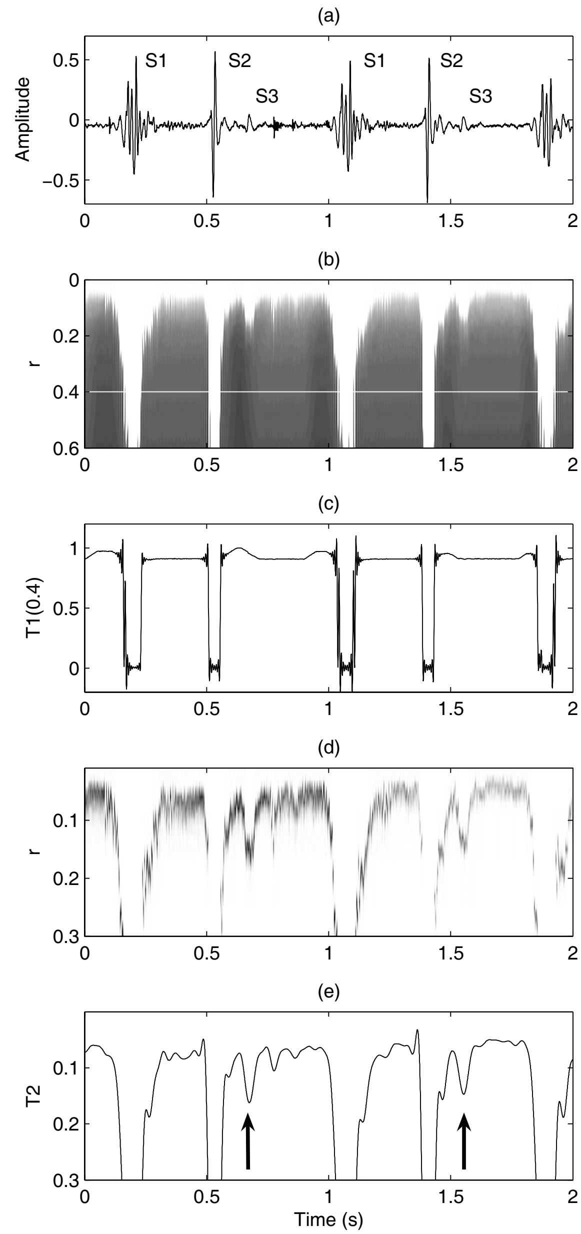


Fig. 3. Example of heart sound signal where the 1$^{st}$, 2$^{nd}$ and 3$^{rd}$ heart sounds are marked as S1, S2 and S3 (a). T1, calculated for a range of r-values, is shown in (b) while a single T1 is shown in (c) for r = 0.4. T1(0.4) is used to find the 1$^{st}$ and 2$^{nd}$ heart sound. T2, calculated for a whole range of r-values is shown in (d). An edge detection algorithm is used to convert T2 to the 1D signal in (e) which is used to detect S3 (marked as arrows by the detection algorithm).

Comparing the results from this method with the tailored wavelet approach in [2, 3] shows some important differences. This method gives a higher detection rate (98 % compared to 93 %), at the expense of a higher amount of false detections (7 % compared to 2 %). A combination of the two methods, where this approach finds S3 and the wavelet approach excludes false detections, could be beneficial. This is however left for future studies.

There might be complications with the method for patients with arrhythmia, e.g. with extra systoles. However, we did not notice any detection problems for normal heart rate variations. Investigation of pathophysiological phonocardiograms is left for future studies.

## 5. CONCLUSION

A novel method for detection of 3rd heart sounds has been developed. The algorithm exploits differences in a reconstructed state space to detect signal transitions with very low energy. A recurrence time statistic is used as a measure to quantify the changes. The method is capable of detecting S3 with high accuracy and robustness. Compared to previous methods, the detection rate is better. However, the amount of false detections is also a bit higher.

## ACKNOWLEDGMENT

This work was supported by the Swedish Agency for Innovation Systems and the Swedish Research Council.

## 6. REFERENCES

[1] N. J. Mehta and I. A. Khan, "Third heart sound: genesis and clinical importance," *Int J Cardiol*, vol. 97, pp. 183-186, 2004.

[2] P. Hult, T. Fjallbrant, K. Hilden, U. Dahlstrom, B. Wranne, and P. Ask, "Detection of the third heart sound using a tailored wavelet approach: method verification," *Med Biol Eng Comput*, vol. 43, pp. 212-217, 2005.

[3] P. Hult, T. Fjallbrant, B. Wranne, and P. Ask, "Detection of the third heart sound using a tailored wavelet approach," *Med Biol Eng Comput*, vol. 42, pp. 253-258, 2004.

[4] N. Joshi, "The third heart sound," *South Med J*, vol. 92, pp. 756-761, 1999.

[5] L. G. Durand and P. Pibarot, "Digital signal processing of the phonocardiogram: review of the most recent advancements," *Crit Rev Biomed Eng*, vol. 23, pp. 163-219, 1995.

[6] P. Hult, "Bioacoustic Principles used in Monitoring and Diagnostic Applications," in *Linköping University*, Ph.D. Thesis, 2002.

[7] H. Kantz and T. Schreiber, *Nonlinear time series analysis*, 2. ed. Cambridge: Cambridge Univ. Press, 2004.

[8] T. Sauer, J. A. Yorke, and M. Casdagli, "Embedology," *Journal of Statistical Physics*, vol. 65, pp. 579-616, 1991.

[9] J. B. Gao, "Recurrence time statistics for chaotic systems and their applications," *Physical Review Letters*, vol. 83, pp. 3178-3181, 1999.

[10] J. B. Gao, Y. H. Cao, L. Y. Gu, J. G. Harris, and J. C. Principe, "Detection of weak transitions in signal dynamics using recurrence time statistics," *Physics Letters A*, vol. 317, pp. 64-72, 2003.